Pergamon

0301-9322(94)E0007-6

Int. J. Multiphase Flow Vol. 20, No. 2, pp. 445–452, 1994

0301-9322/94 $7.00 + 0.00

BRIEF COMMUNICATION

SEDIMENTATION OF COMPLEX-SHAPED PARTICLES IN A SQUARE TANK AT LOW REYNOLDS NUMBERS

V. ILIC and J. VINCENT
Department of Mechanical Engineering, University of Sydney, Sydney, NSW 2006, Australia

(Received 14 June 1993; in revised form 8 August 1993)

INTRODUCTION

In spite of its industrial relevance, sedimentation of non-spherical particles at low Reynolds numbers (Re) has not been well-documented in the open literature. By contrast, the sedimentation of spherical particles, either singly or in clusters, is now well-documented and understood and has been modelled accurately with the boundary element method (BEM) for about 20 years (Youngren & Acrivos 1975).

Early systematic experimental studies of the sedimentation of single, geometrically regular complex shapes include those by Pettyjohn & Christiansen (1948), McNown & Malaika (1950) and Heiss & Coull (1952). They recognized, among other things, the influence of container boundaries on the settling velocity of complex-shaped particles, as well as the effect of their aspect ratio.

Coutanceau (1987) also examined the wall effect, but for various particle shapes based on a two-dimensional polynomial equation for the equatorial plane of the particle. Jayaweera & Mason (1965) related the stability of sedimenting cones to their apex angle. However, these studies omitted to relate the settling velocity of a complex-shaped particle to that of a sphere on the basis of equal surface area or volume, such that the shape effect could be unambiguously determined.

This experimental study aimed appropriately to isolate the effect of a variety of particle shapes on their settling velocity at low Re in a fluid column of square cross-section. The chosen fluid was an isothermal, incompressible, Newtonian liquid and the test particles had either equal surface areas or volumes.

A comparison of these data with the BEM predictions was also sought as a benchmark for future numerical modelling.

The work reported here is restricted to solid particles of regular complex shape, having a stable orientation, equal surface areas or volumes and settling at terminal velocity along the geometrical axis of the test tank. The size of the particles was such that hydrodynamic effects predominated.

METHOD

Test shapes, the conduit and liquid

The test particle shapes used were a cone, cube, disc, double cone, double pyramid, double tetrahedron, hemisphere, long cylinder, pyramid, sphere, spheroid and a tetrahedron, figure 1. Their dimensions were based on the surface area or volume of a 20 mm dia sphere. Details of their dimensions, masses and release orientations are given in table 1.

Experiments were done in a square conduit (200 × 200 × 900 mm) made from 10 mm thick (fish tank) glass plates. The upper end of this tank accommodated a removable lid containing the test particle releasing fixture, ensuring precise and repeatable location of the drops along the

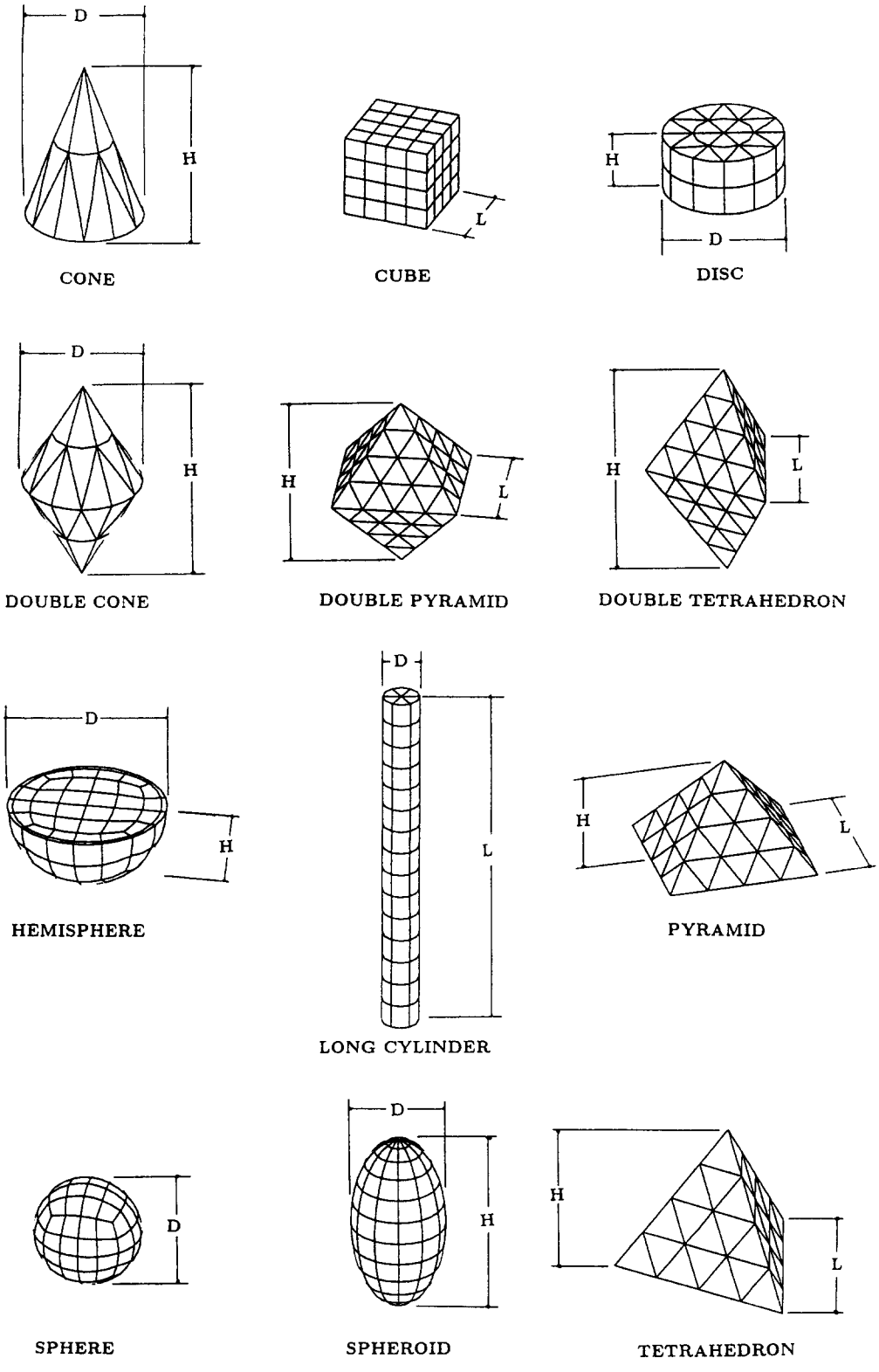

Figure 1. The different shaped particles used in the experiments and the numerical modelling. The quadratic boundary element meshes used are shown. The corresponding geometric details and masses are given in table 1(a) for particles with the same surface area as a 20 mm dia sphere and in table 1(b) for particles with the same volume as a 20 mm dia sphere.

Table 1. Sedimenting particles' mass, dimensions[a] and fall orientation

(a) Aluminium particles with the same surface area as a 20 mm dia sphere

Shape	Mass (g)	Length L (mm)	Diameter D (mm)	Height H (mm)	Orientation
Cone	8.5526		20.05	28.35	Apex up
Cube	8.1624	14.50			Face up
Disc	8.8940		20.05	10.00	Face up
Double cone	10.3103		20.00	34.65	Long axis vertical
Double pyramid	9.9512	19.70		27.65	Long axis vertical
Double tetrahedron	7.0738	21.60		35.50	Long axis vertical
Long cylinder	5.2009	61.75	6.15		Long axis vertical
Long cylinder	5.2097	61.70	6.20		Long axis horizontal
Pyramid	7.0323	22.20		15.10	Apex up
Sphere	11.9276		20.00		
Spheroid	10.8310		15.50	31.00	Long axis vertical
Tetrahedron	6.5293	26.60		21.80	Apex up

(b) Aluminium particles with the same volume as a 20 mm dia sphere

Shape	Mass (g)	Diameter D (mm)	Height H (mm)	Orientation
Cone	12.1899	20.00	40.16	Apex up
Disc	11.7792	19.99	13.31	Face up
Double cone	12.3185	20.02	39.88	Long axis vertical
Hemisphere	11.9837	25.14	12.59	Face up
Long cylinder	11.9287	8.10	81.21	Long axis vertical
Long cylinder	11.8257	8.08	81.18	Long axis horizontal
Sphere	11.8952	19.95		
Spheroid	11.9241	15.86	31.69	Long axis vertical

[a]Dimensions L, D and H are defined in figure 1.

vertical axis of the tank. A spirit level and a plumbline were used to ensure alignment of the tank with the vertical. The start and finish of a settling particle's traverse between two timing marks (inscribed on the exterior walls of the tank) were recorded with two video cameras. These lines were 100 mm apart and just above the half height of the tank. Each camera was levelled with the aid of an in-built spirit level and focused at one of the timing marks such that it was in the centre of its field of view. The depth of field was such that a particle descending along the tank axis was also in sharp focus.

The Newtonian test liquid was Gensil 150/12500 polydimethylsiloxane (a silicone oil), manufactured by Rhône-Poulenc Silicones Australia Pty Ltd, with a specific gravity of 0.974 and a viscosity of 14.5 Pa s at 20.0°C.

The Newtonian nature of the test fluid was ascertained up to shear rates of $34\,s^{-1}$ with an Instron 3250 rheometer.

The test liquid temperature was determined by the environmentally controlled laboratory atmosphere, to within 0.5°C during an experiment. The corresponding change in the liquid viscosity was within the accuracy of its measurement, and hence was neglected in the calculations. The measured temperature difference over the liquid column length was small and of the order of the resolution (0.1°C) of the temperature indicator, and was considered negligible.

Apparatus, data collection and processing

At the start of an experiment, the particle to be dropped was held by vacuum in the required position in the test conduit fixture attached to the cylinder lid and, prior to its release, was partially immersed in the tank liquid.

Two single CCD (charge coupled device) chip video cameras (Panasonic WV-BL200) with 420 horizontal line resolution at the centre, were each fitted with a Computar lens ($f = 1{:}1.2$, 12.5–75 mm zoom) and focused at timing marks on the outside of the conduit. The cameras were mutually orthogonal to detect any particle trajectory deviations away from the vertical centreline of the tank, and each conveyed a signal to a video splitter (American Dynamics 1470 A). The video splitter was used to provide a simultaneous view of the two images on the monitor screen (National WV-5410E/A), whose resolution was more than 850 lines at the centre. The displayed combined image was recorded on an SVHS VCR (Panasonic NVFS 100A). The test time

(to two-hundredths of a second) from the National time generator WJ-810 was superimposed on the combined image.

The test procedure was to put the test particle in the locating fixture attached to the tank lid, switch on the vacuum pump to hold it in place and cap the test tank. As the VCR was switched from "hold" to "record" mode, the vacuum pump was stopped, releasing the partially immersed particle. The "record" mode was switched to "hold" once the particle went past the lower timing mark. This procedure was repeated for all the particles used in the test.

Following the drops, the video tape was rewound and the VCR "single frame advance" mode activated until the test particle "touched" the top timing mark. The time record was then read off the video frame. This was repeated for the lower timing mark. A particle terminal velocity was then determined from the known distance between the two timing marks on the test cylinder and the corresponding time interval.

It is estimated that the experimental error for the settling velocity is $<2\%$ on the basis of the uncertainties in the measurements of time and distance.

Numerical implementation

For the fluid BEM modelling (Tullock 1993), 88 elements were used on the tank and between 24 and 96 on the particles. All the elements were quadratic in geometry, traction and velocity variation.

Numerical evaluations of a particle settling velocity were done on a Stardent Titan work station and typically required 2000 s CPU time to obtain a solution.

RESULTS AND DISCUSSION

General

All tests reported here were done for sufficiently low particles' Re (range 0.003–0.047), such that the Stokesian flow analysis of the data is appropriate.

It was observed that not all particles maintained their initial orientation during the fall. The pyramid, cone and tetrahedron showed a preference to fall with their apex uppermost. This instability was also observed by Jayaweera & Mason (1965), who found that the orientation preference depended on a particle's apex angle. The double pyramid, double cone, double tetrahedron and long cylinder were stable when released with their longest axis of symmetry coaxial with the axis of the tank. The long cylinder was also stable when released with its axis normal to the drop. The cube was released with a face downward. The data reported here refer only to the stable sedimentation configurations over the measuring region (near the middle height of the test tank).

The results are shown in figures 2–4. The experimental and BEM results are shown together for comparison in figures 2 and 3. As expected, a close agreement between the numerical and experimental data is generally apparent, indicating that the BEM is a good modelling tool for the settling velocity, at low Re, of regular complex-shaped particles falling in a quiescent column of an isothermal, incompressible, Newtonian liquid having a square cross-section.

Particles of equal surface area

Results for different shaped particles with equal surface areas are shown in figure 2. The ordinate represents a particle's terminal velocity normalized with the terminal velocity of a sphere, having the same surface area and density as the particle, settling in the same tank. The sphere velocity was 2.16 cm/s at the liquid temperature of 20.8°C. As expected, particles with the largest volume per unit surface area (the sphere and the double cone) fell faster than those with the smallest (the long cylinder), regardless of the particle shape.

Therefore, the concept of an equivalent sphere was devised to extract from the data the influence on the settling velocity, of the shape only. The dashed line represents the calculated normalized velocity of a sphere having the same surface area as any particle here with a force applied to it corresponding to that acting on any given volume on the abscissa. A particle's

vertical distance from this line therefore represents the influence of its shape, relative to an equivalent sphere, on its settling velocity rather than that of its surface area or propulsive force. For shapes whose projected area is concentrated close to the particle vertical axis (unlike that of the long cylinder with its axis horizontal), this shape effect is observed to be about 15% maximum (for the double tetrahedron). This observation is reinforced by the fact that the numerical and experimental values coincide here.

An implication of this result is that, as a first approximation, the Stokes equation could be used directly to evaluate the settling velocity of a complex-shaped particle represented as an *equivalent* sphere. The result obtained should be to within 15% of the correct value. This observation is to be contrasted against a discrepancy of up to 50% for a sphere of the same surface area and density.

As can be seen from the figure, the agreement between the numerical and experimental data is generally within 2% for all the shapes except the cube, for which the numerical prediction is approximately 9% greater than the experimental result. This discrepancy is probably caused by a slight change in the cube's orientation during the experiment.

Particles of equal volume

The behaviour of different shaped particles with equal volumes, and therefore of equal applied forces, is shown in figure 3. The ordinate in this figure represents the terminal velocity of a settling particle normalized with the terminal velocity of a sphere of the same volume and density. Again, the expected result is observed: for particles with equal volumes, the sedimentation velocity is inversely related to a particle's surface area; the sphere, having the least surface area for a given volume, has the greatest velocity, while the long cylinder of equal volume (and aspect ratio of 10:1) has the largest surface area of all the particles tested, and hence has the smallest settling velocity. As in the case for particles with equal surface areas, the concept of an equivalent sphere is therefore introduced to isolate the effect of particle shape, relative to this sphere, on the settling velocity.

The dashed line represents the calculated settling velocity of a sphere with the same applied force as any particle here but with a surface area corresponding to a given point on the abscissa. The shape effect is observed to be about 6% maximum (for the double cone). It should be noted that the numerical and experimental data for the double cone actually coincide after the mass correction [it is about 3.6% greater than the sphere of equal volume, table 1(b)].

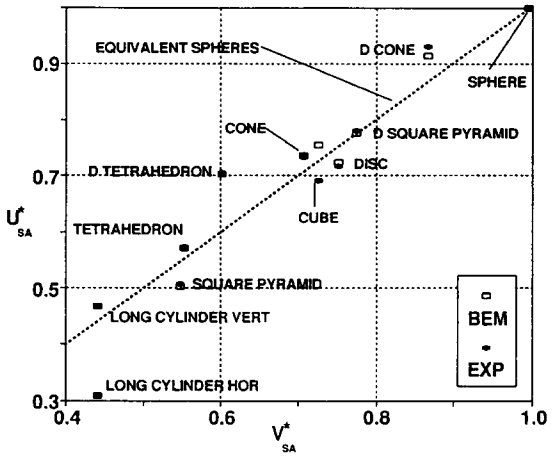

Figure 2. The sedimentation velocities for particles with the same surface area. U^*_{SA} denotes the settling velocity of the particle normalized with the velocity of a sphere of the same surface area as the particle; V^*_{SA} denotes the particle volume normalized against the volume of a sphere of equal surface area. The dashed line represents the calculated velocity of a 20 mm dia sphere with a force applied to it corresponding to a given volume on the abscissa.

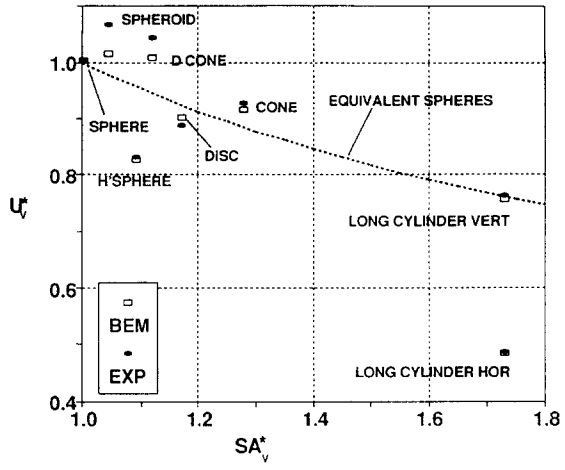

Figure 3. The sedimentation velocities for particles with the same volume. U_V^* denotes the settling velocity of the particle normalized with the velocity of a sphere of the same volume as the particle; SA_V^* denotes the particle surface area normalized against the surface area of a sphere having the same volume as the particle. The dashed line represents the calculated velocity of a sphere whose surface area corresponds to a given surface area on the abscissa with an applied force equal to that of any given particle.

Particles of different volumes and surface areas

Experimental results for different shaped particles with different surface areas and volumes are shown in figure 4. Each particle's velocity has been normalized with that of a sphere having a surface area and applied force equal to that of the particle, thus eliminating the effects of surface area and propulsive force on the velocity and leaving only the effect of the particle's shape.

For particles with projected area (PA_{SA}^*) in the range 0.6–1.5, an interesting observation here is the occurrence of the three linear relationships (depending on a particle's generic form) denoted by dashed lines in figure 4. The first, for particles with a symmetrical point at each end, vertically in line and in the direction of fall; these have the highest settling velocities. The second, for particles with a point at one end and a flat (horizontal) face at the opposite end; these were found to have moderate velocities. And the third, at an even lower velocity for those which are flat at both ends and whose flats are horizontal and normal to the direction of fall.

It is also interesting that the three lines appear to converge, suggesting that, for a given particle surface area, increasing its projected area diminishes the effect of geometrical differences on the

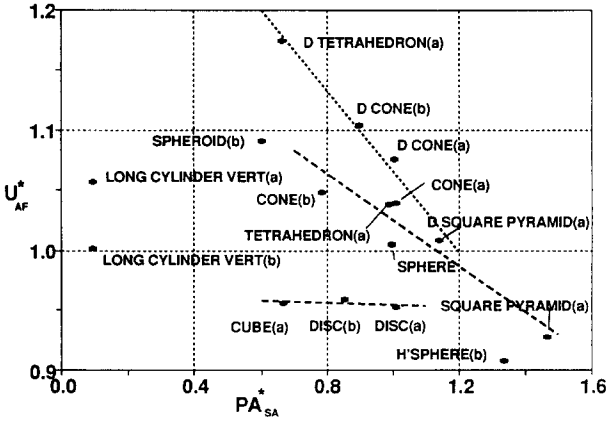

Figure 4. Variation of particle velocity with projected area. U_{AF}^* denotes the particle settling velocity normalized against the velocity of a sphere with the same surface area and applied force; PA_{SA}^* denotes the particle vertical projected area normalized against the projected area of the sphere having the same surface area as the particle. Particle details are given in tables 1(a) and 1(b), indicated in parentheses adjacent to a particle designation.

Table 2. Variations of the Stokes wall effect factor ($K = U_\infty/u$) for PA^*_{SA} for complex-shaped particles having the same surface area or volume (v) as a 20 mm dia sphere

Shape	PA^*_{SA}	K	K/K_{sphere}	Orientation
Cone	1.0073	1.24	1.008	Apex up
Cube	0.6675	1.22	0.992	Face up
Disc	1.0073	1.24	1.008	Face up
Double cone	1.0053	1.26	1.024	Long axis vertical
Double pyramid	1.1405	1.25	1.016	Long axis vertical
Double tetrahedron	0.663	1.20	0.976	Long axis vertical
Long cylinder	0.0951	1.21	0.984	Long axis vertical
Pyramid	1.4656	1.26	1.024	Apex up
Sphere	0.9968	1.23	1.000	
Tetrahedron	0.9889	1.21	0.984	Apex up
Cone (v)	0.7854	1.27	1.033	Apex up
Disc (v)	0.8549	1.26	1.024	Face up
Double cone (v)	0.8976	1.27	1.033	Long axis vertical

settling velocity. It can easily be shown that the maximum value that the abscissa can have for a physical particle is 2.0 and that any particle having this value will be reduced to a two-dimensional lamina.

The conventional Stokes wall correction factor K (the calculated velocity of a particle in an unbounded fluid U_∞, relative to the measured velocity, u) varies very little between the different particles, table 2. This is probably the result of the very small difference in the particle sizes (their surface and projected areas) relative to the cross-sectional area of the tank.

Furthermore, it is also apparent from the variation of K/K_{sphere} in table 2 that the normalizing effect of the sphere in figures 2–4 effectively eliminated (to within 3.3%) the effect of the wall proximity on a particle's settling velocity.

SUMMARY AND CONCLUSIONS

For the Re range 0.003–0.047, the steady-state settling velocities of complex-shaped particles were studied experimentally and benchmarked numerically using the BEM.

The particles were made from aluminium and had their surface area or volume equal to that of a 20 mm dia sphere. All particles were released singly at the axis of symmetry of a 200 × 200 mm square tank containing a Newtonian fluid (a silicone oil: polydimethylsiloxane).

- For PA^*_{SA} in the range 0.6–1.5, irrespective of the particles' surface areas or volumes, there was a tendency for grouping related to particles' longitudinal symmetry: shapes with pointed ends settled faster (per unit force) than those with flat end surfaces. The sphere and particles with one flat and one pointed end had an intermediate settling velocity.
- From the slope of the regression lines for the three particle categories it is also apparent that, for a given particle surface area, the effect of geometrical differences on the settling velocity is diminishing with increasing particle normalized PA^*_{SA}.
- It was also found that, for the variety of complex shapes, there was a maximum deviation of about 15% in the settling velocity of a particle from the velocity of an equivalent sphere. This implies that, as a first approximation, the settling velocity of a complex-shaped particle could be obtained directly from the Stokes law, via the *equivalent* sphere concept. The value so obtained should be to within 15% of the true value.
- The Stokes wall correction factor, defined as the ratio of the Stokes velocity to the measured velocity of a particle, was found to be about 1.2 and approximately independent of the particle shape for the range of experimental parameters used.
- As expected, the experimental sedimentation data are well-described (generally, to within 2%) with the fully three-dimensional BEM, indicating that numerical

experiments with non-spherical particles sedimenting in a tank of square cross-section, can now be carried out with confidence.

Future sedimentation studies on complex-shaped particles should address in detail the problem of orientational stability, as well as inter-particle and particle–wall interactions, and especially the role of the particle aspect ratio in these. Extension of this work to sedimentation in non-Newtonian fluids is also of practical interest.

Acknowledgements—We are grateful to Professors R. I. Tanner and N. Phan-Thien for their helpful comments and general guidance throughout the course of this study. We thank Alcan Australia Ltd, Artel Industries Ltd (New Zealand), Rhône-Poulenc Silicones Australia Pty Ltd, BP Chemicals Ltd, Goodman Fielders Mills Ltd, Oral-B Laboratories Pty Ltd, RMAX of Pacific Dunlop Ltd and Tioxide Australia Pty Ltd for their support in kind. This work was funded in part by a Sydney University Special Projects Grant.

REFERENCES

COUTANCEAU, M. 1987 Confined creeping flow around an axisymmetric body: increase of the shape effect by a tube wall. *Fluid Dynam. Res.* **2,** 153–174.

HEISS, J. F. & COULL, J. 1952 The effect of orientation and shape on the settling velocity of non-isometric particles in a viscous medium. *Chem. Engng Prog.* **40,** 133–140.

JAYAWEERA, K. O. L. & MASON, B. J. 1965 The behaviour of freely falling cylinders and cones in a viscous fluid. *J. Fluid Mech.* **22,** 709–720.

MCNOWN, J. S. & MALAIKA, J. 1950 Effects of particle shape on settling velocity at low Reynolds numbers. *Trans. Am. Geophys. Union* **31,** 74–82.

PETTYJOHN, E. S. & CHRISTIANSEN, E. B. 1948 Effect of particle shape on free-settling rates of isometric particles. *Chem. Engng Prog.* **44,** 157–172.

TULLOCK, D. L. 1993 New developments and applications of the boundary element method for some problems in elasticity and viscous flow. Ph.D. Thesis, Dept of Mechanical Engineering, Univ. of Sydney, NSW.

YOUNGREN, G. K. & ACRIVOS, A. 1975 Stokes flow past a particle of arbitrary shape: a numerical method of solution. *J. Fluid Mech.* **69,** 377–403.